Spring 5-6-2012

Evidence for PiT-Type (SLC20) and NaPi-II-Type (SLC34) Transporters in the Rat Choroid Plexus

Hien M. Le
University of Connecticut - Storrs, hien.m.le@gmail.com

Evidence for PiT-Type (SLC20) and NaPi-II-Type (SLC34) Transporters in the Rat Choroid Plexus

Hien M. Le

PNB 4296W

University Scholar and Honors Thesis

May 2012

TABLE OF CONTENTS

LIST OF TABLES AND FIGURES

ABSTRACT

A major function of the brain choroid plexus (CP) is to regulate the exchange of solutes between the blood plasma and the cerebrospinal fluid (CSF) using selective transporters. CSF inorganic phosphate (P_i) concentration is maintained at about one-half that of plasma and is potentially important because of its regulatory, structural, and biochemical functions. Phosphate is critical for ATP and DNA formation, the linked regulation between phosphate and calcium, and as an intracellular buffer. The human body has two major P_i transporter gene families known as SLC34 (NaPi-II) and SLC20 (PiT), which have wide tissue distribution. Although both families are secondary-active and sodium-dependent, they are distinguished by their transport mechanisms and functional properties. NaPi-II-type and PiT-type transporters are characterized by their substrate stoichiometry and inhibition profile. Unlike NaPi-II-type transporters, PiT-type transporters are not inhibited by phosphonoformic acid (PFA) and can partially substitute Li^+ for Na^+. Bataille et al. (unpublished) used these differences to characterize the effects of arsenate, PFA, and Li^+ on CP phosphate transport. The results indicate that a PiT-type transporter is responsible for P_i transport in the CP. To further support this hypothesis, RT-PCR and western blotting were performed to definitively determine if NaPi-II-type transporters are present or absent from the CP. The results confirm the presence of PiT-like transporters but also indicate that NaPi-IIb is potentially present in the CP. Thus, the secondary-active, CP transport of phosphate out of the CSF may involve more than one family of solute carrier transporters.

1. INTRODUCTION

1.1 The Choroid Plexus and CSF Formation

Also known as the "kidney of the brain," the choroid plexus (CP) tissues are interventricular organ that secrete two-thirds of total cerebrospinal fluid and mediate the transport of solutes between the blood plasma to the cerebrospinal fluid (CSF) (10, 32). The CP is divided into four parts with tissues in each lateral ventricle, third ventricle, and fourth ventricle, as seen in Figure 1(28). CP tissue is comprised of a continuous monolayer of cuboidal and columnar epithelial cells that is situated on connective tissue (Figure 2). The lateral ventricles of the mammalian brain have sheet-like choroid plexus structures, whereas the choroid plexuses in the third and four ventricles are branched villi that protrude into the ventricle (7). Each villus has a central vascular axis that is covered by ciliated cuboidal epithelium with numerous mitochondria. The epithelium also contains dendritic cells, which suggests that the CP may play in active role in immunological brain protection (28).

The CP is paired with the fenestrated endothelium of the cerebral capillary beds to form the blood-CSF barrier (Figure 3) (10). The epithelium layer folds into numerous small villi to increase surface area and is designated as the major barrier of substrate movement between the blood and CSF (7). One of the CP's major functions is to transport essential CSF electrolytes, such as Na^+, Cl^-, HCO_3^-, K^+, and the topic of this report, inorganic phosphate (P_i), across its epithelium (32). In addition to epithelial transport, the CP is responsible for the majority (two-thirds) of total CSF production. Extrachoroidal sites make up the latter third of total CSF production with less than 10% of total CSF formation coming from brain interstitial fluid and the rest originating from water produced in the brain cells by glucose oxidation and ultrafiltration across the cerebral microvessels (23). The rate of CSF production is relatively high compared to

total human CSF volume (150-170 mL), suggesting that CSF is constantly renewed and old fluid is removed by bulk flow. Over a 24 hour period, it has been estimated that ~600 mL of CSF is produced, a large enough volume to replace existing CSF three to four times (23). CSF production begins with passive filtration of fluid across choroidal capillary endothelium followed by active secretion across the CP (10).

The role of the CP in CSF production is important because the CSF physically and chemically protects the brain. The buoyancy of CSF reduces the weight of the brain nearly 30-fold, from 1,500 grams to approximately 50 grams. This translates into a decreased pressure on blood vessels and nerves attached to the CNS. Moreover, the buoyant nature of CSF prevents the cerebrum from crushing the brainstem and serves as a mechanical buffer to protect the CNS from damage caused by physical impact to the skull (7, 23, 29). To maintain a stable environment within the intraventricular milieu, CSF is constantly secreted which then displaces older fluid. This is important because the brain lacks lymphatic capillaries, and CSF flow assists in the removal of waste products, debris, bacteria, and viruses (10, 29). CSF flow starts within the ventricle cavities, into the subarachnoid space, and finally drains into the systemic circulation via the dural sinuses (Figure 4) (7, 29). The fluid flows unidirectionally due to the presence of valve-like mechanisms to prevent the regurgitation of blood into the subarachnoid space (6).

Because of the brain's special metabolic requirements, the composition of CSF is vital to brain health. Neurons require a constant glucose and oxygen supply for ATP synthesis to fuel active transport of ions and neurotransmitters. Thus, the brain receives 15% of the blood pumped by the heart (29). To illustrate the importance of the choroid plexus, the blood flow to the CP is 10 times higher than the blood flow to the brain parenchyma and five times higher than the blood flow to the kidney, on a per gram basis. The adult human CP secretes the equivalent of 10% of

the received blood flow or approximately 0.5 liters/day. Despite fluctuations in blood flow and pressure, the CP is remarkable at balancing CSF production and reabsorption to maintain an intracranial pressure between 5-15 mm Hg above that of the arterial blood. Moreover, the CP is extraordinary at keeping CSF composition constant over time despite changes in the blood compartment. For instance, CSF [K^+] increases by less than 2 mM when plasma [K^+] changes from 1.6 to 11 mM (7). The ability to finely control CSF formation has been a challenge but is clinically important due to its relation to brain fluid disorders such as congenital hydrocephaly. Congenital hydrocephalus is one of the most common birth defects, affecting up to 1 in 500 births and is severe because it disrupts brain development, which ultimately decreases neurogenesis (13). Most attempts to regulate CSF formation are focused on altering ion movement via transporters in the membranes of CP epithelium (10).

1.2 Phosphate in Physiological Systems

P_i is an essential dietary nutrient that is absorbed from food as an electrically charged salt anion. In fact, phosphorus is the sixth most abundant element in the body (9). Approximately 85% of P_i in the body is found in the bones, 14% is in the cells of soft tissues, and the remaining 1% is in extracellular fluids (16). Extracellular [P_i] must be stable at ~1.1 mM for proper cellular function (18). The CSF has a P_i concentration held between 0.5 mM and 1.0 mM, whereas the plasma has a [P_i] range between 1.5 to 1.8 mM (2). The reason for the lower CSF [P_i] relative to plasma [P_i] is unexplained.

Every cell requires P_i for structural, metabolic, and regulatory purposes. Examples of cellular structures that incorporate phosphate are the DNA backbone, phospholipids in the cell membranes, and phosphoproteins that are necessary for mitochondrial function. Moreover, important intracellular compounds such as cyclic adenine and the enzymatic co-factor

nictoniamide diphosphate are dependent on intracellular phosphate pools for their formation (24).

Another physiological function of phosphate is the regulation of intracellular processes, such as protein, fat, and carbohydrate metabolism. Phosphorylation is a major regulatory process that may directly modulate numerous enzymatic reactions, including glycolysis and ammoniagenesis. P_i seems to have its most obvious role as the source of the high-energy bonds in ATP. The energy stored in ATP provides the energy for vital physiological processes such as muscle contractility and electrolyte transport (29). Because of ATP's various functions within the cell, P_i is an indicator of cellular metabolic capability.

P_i is a triprotic acid and it loses its three hydrogen's sequentially (29):

1. $H_3PO_{4\,(aq)} \leftrightarrow H^+_{(aq)} + H_2PO_4^-{}_{(aq)}$
2. $H_2PO_4^-{}_{(aq)} \leftrightarrow H^+_{(aq)} + HPO_4^{2-}{}_{(aq)}$
3. $HPO_4^{2-}{}_{(aq)} \leftrightarrow H^+_{(aq)} + PO_4^{3-}{}_{(aq)}$

Physiological P_i is present in two forms $H_2PO_4^-$ and HPO_4^{2-} and is a nearly ideal physiological buffer, as represented by equation 2 and evident by its 7.21 pK_a (6). Eighty percent of plasma P_i is in the divalent form at physiological pH, which is slightly alkaline at 7.38-7.40 . H^+ concentrations must be tightly regulated because dramatic changes in pH will disrupt the protein's tertiary structure, leading to dysfunction. In the CNS, pH fluctuations may cause dire consequences. Acidosis can result in less excitable neurons and ultimately CNS depression. Patients exhibiting CNS depression are confused and disoriented and can potentially slip into a coma. If CNS depression continues, the respiratory centers fail, resulting in death. On the other hand, if the pH is too high, alkalosis causes neurons to become hyperexcitable, initiating action potentials at the slightest signal. At first, the condition clinically presents itself as sensory changes, such as numbness or tingling, and subsequently as muscle twitches (29). To prevent

these disorders, buffers are used as a first line of defense. The most common intracellular buffers are proteins and notably, P_i. Unlike plasma, CSF has an almost complete lack of protein (less than 0.5 g/L), yet the CSF pH is very stable. Changes in the concentration of plasma HCO_3^- have little effect on CSF [HCO_3^-]. However, an elevation in blood P_{CO2} results in an increase in CSF P_{CO2} but not as high as predicted. Thus, there must be some sort of mechanism that regulates pH, and P_i is a potential candidate to explain this phenomenon. Interestingly, a 0.05 unit drop in CSF pH causes a 10-fold increase in ventilation rate (7).

Varying P_i concentrations influence Ca^{2+} concentrations. Their regulation is linked which is further supported by the contribution of several organs and hormones that control both their concentrations. Intestinal absorption, bone (de)mineralization, and renal reabsorption/excretion are all affected by the same hormones that increase or decrease plasma [Ca^{2+}] or [P_i]. For example, parathyroid hormone (PTH) increases plasma [Ca^{2+}] by enhancing renal reabsorption and decreasing plasma [P_i] by increasing renal excretion. PTH also causes the mobilization of calcium from bones, resulting in a release of P_i (24). This is because 99% of Ca^{2+} and P_i are found in the bones in the form of hydroxyapatite, $Ca_{10}(PO_4)_6(OH)_2$ (19, 29). Although it is unknown whether hormones influence CP P_i transport, it is still pertinent to consider the effects of P_i on Ca^{2+} concentrations.

The relationship between P_i and Ca^{2+} concentrations is relevant because of the several physiological functions of calcium. Cells use calcium for intracellular signaling to initiate a variety of essential processes. For example, calcium initiates the exocytosis of synaptic and secretory vesicles and the contraction of muscle fibers. If plasma Ca^{2+} levels are not tightly controlled, neuron excitability can be induced. Hypocalcemia increases neuronal permeability to

Na^+, causing neuronal depolarization and CNS hyperexcitability. On the other hand, hypercalcemia, causes neuromuscular depression (29).

1.3 Phosphate Transporters: SLC20 versus SLC34

Cells acquire P_i from extracellular fluid by secondary-active transport. P_i transporters drive P_i influx by utilizing the inwardly directed electrochemical Na^+ gradient formed by Na^+-K^+-ATPase. The two major P_i transporters are called NaPi-II (SLC34) and PiT (SLC20) and are similar in that they are both secondary active and Na^+-coupled (33). However, the two solute protein carriers are distinguished by their mechanistic properties and physiological roles.

SLC34 Transporter Family

The type II Na/P_i protein has three isoforms known as NaPi-IIa (SLC34A1), NaPi-IIb (SLC34A2), and NaPi-IIc (SLC34A3). P_i transporters from the SLC34 gene family are most highly expressed in the small intestine and in the renal proximal tubules, the two most important sites for controlling systemic P_i concentrations (18). The importance of the SLC34 transporter family is conveyed by the hyperphosphaturia, hypophosphatemia, and increased renal stone incidence documented in NaPi-IIa ($Npt2a^{-/-}$) knockout mice and the presence of osteoporosis and nephrolithiasis in heterozygous mutated NaPi-IIa mice ($Npt2a^{+/-}$) (20, 33).

NaPi-II isoforms are differentially expressed throughout the body. Specifically, NaPi-IIa transporters have been found in bone and kidney, NaPi-IIb transporters are expressed in enterocytes and lung tissue, and NaPi-IIc transporters are exclusively seen in the kidney (18). All NaPi-II isoforms prefer the divalent P_i and are strictly dependent on Na^+. An important difference between SLC20 and SLC34 is that the latter is inhibited by phosphonoformic acid (PFA), which makes NaPi-II identifiable during transport studies (33).

NaPi-IIa-type transporters are an 80-90 kDa protein that is principally localized in the microvilli that make up the brush border membrane of the renal proximal tubule. NaPi-IIa transport cycles are electrogenic and characterized by an inward transfer of one net positive charge per cycle. Three Na^+ ions and one HPO_4^{2-} bind to the NaPi-II protein in a $Na^+/P_i/Na^+$ ordered manner, with substrate affinities of K_m^{Pi} ~0.1 mM and K_m^{Na} ~70 mM. Transport rates are higher at more alkaline external pH values (18). Targeted type IIa knockout mice have demonstrated that NaPi co-transport in brush-border membrane vesicles is reduced by 70%, indicating that most proximal tubule P_i is by NaPi-IIa transporters (16).

NaPi-IIb mRNA expression has been identified in a variety of tissues that include the lung, small intestines, testis, mammary glands, and the liver. Immunofluorescence has indicated that NaPi-IIb-type transporters are localized to the brush borders of enterocytes and the apical membrane of alveolar type II cells. The fully glycosylated 108 kDa protein transports in an electrogenic, 3Na: $1P_i$ stoichiometric fashion and has a binding affinity of K_m^{Pi} <50 μM and K_m^{Na+} ~40 mM. There is moderate pH dependence, with a slightly higher co-transport at more acidic pH values (18). Although western blots have detected glycosylated proteins at 108 kDa, NaPi-IIb transporters have been observed to only be partially glycosylated in weaning animals (18). NaPi-IIb ($Npt2b^{+/-}$ and $Npt2b^{-/-}$) knockout mice have been phenotypically analyzed and all $Npt2b^{-/-}$ mice died in utero, suggesting that NaPi-IIb-type transporters are essential for early embryonic development. In contrast, weaning hetero $Npt2b^{+/-}$ mice display hypophosphatemia and hypophosphaturia. Moreover, Ohi et al. showed that $Npt2b^{+/-}$ mice with adenine-induced renal failure had decreased plasma P_i levels compared with the level in $Npt2b^{+/+}$ mice. These knockout studies demonstrate that NaPi-IIb is important as a therapeutic target for the prevention of hyperphosphatemia and is a regulator of systemic P_i homeostasis (19).

The last SLC34 isoform, NaPi-IIc, is found exclusively on the apical membranes of the proximal tubules of the deep nephrons. In contrast to its counterparts, the 75 kDa protein is electroneutral with a transport Na:P_i stoichiometry of 2:1. Substrate affinity is K_m^{Pi} 70 μM and K_m^{Na} 40 mM. NaPi-IIc is highly pH dependent and exhibits a higher transport at more alkaline pH (18, 27). Type IIc NaPi-knockout mice models have shown that it is responsible for residual P_i transport and accounts for 30% of renal P_i reabsorption (16). NaPi-IIc transporters are described as growth related. While the level of type IIa NaPi transporters increase with age, NaPi-IIc protein expression decreases with age and has its greatest expression in weaning animals. In the adult kidney, NapI-IIc transporters are localized to the midcortical region of the adult kidney but are found in the midcortical and superficical region in the kidney of weaning animals. In Npt2a$^{-/-}$ mouse kidneys, NaPi-IIc protein expression increased with age and persisted until adulthood [unpublished observation] (15). The high levels of the type-IIc isoform may compensate for reduced [P_i] transport when NaPi-IIa expression is low to support growth in Npt2a$^{-/-}$ mice.

SLC20 Transporter Family

Also described as retroviral receptors, the SLC20 solute carrier family preferentially transports Na^+ and the monovalent $H_2PO_4^-$. Two isoforms, PiT1(SLC20A1) and PiT2 (SLC20A2) make up the SLC20 family and share ~60% sequence homology (4, 33). The PiT proteins have wide tissue distribution but each isoform is differentially expressed. Unfortunately, there is only limited data on the distribution and subcellular localization of PiT1 and PiT2 proteins. Some precise localization studies have shown that PiT expression in the distal convoluted tubule in the kidney and PiT2 mRNA has been found in epithelial cells along the crypt/villus axis in mouse small intestinal cells. Moreover, PiT1 mRNA has been detected in

osteoclasts and macrophages and transfected PiT1 proteins have localized to the basolateral membrane (33). Although the physiological role of SLC20 proteins has not been definitive, it has been suggested that PiT paralogs are cellular "housekeeping" proteins that maintain cellular P_i homeostasis. This is because SLC20 proteins are likely to have basolateral localization within epithelial cells and there is an upregulation of PiT protein expression when extracellular P_i levels are low (3, 4).

The PiT1 and PiT2 co-transporters specifically mediate the movement of Na^+ and P_i across the cell membrane and have many distinguishing transport mechanisms. Both PiT proteins have a Na^+:P_i transport stoichiometry of 2:1, and because the preferred substrate is $H_2PO_4^-$, their transport is electrogenic. Unlike NaPi-II-type transporters, PiT proteins can substitute Na^+ with Li^+ to support P_i transport. Additionally, two studies have indicated that H^+ can support P_i transport to a small extent in the absence of Na^+. The optimal pH range for PiT1 and PiT2 P_i transport is between 6.2 and 8.0, and lowering the pH from 7.5 to 6.0 significantly increased P_i transport across the cell membrane. This is different from NaPi-II-mediated transport, which is strongly reduced at acidic pH because of the inhibitory effects of H^+ and the decreased availability of HPO_4^{2-}. Thus, PiT proteins are able to transport P_i at pH's as acidic as 5.0 (3, 33).

Another distinguishing characteristic of PiT-mediated transport is the involvement of divalent ions. In the absence of Ca^{2+} and Mg^{2+}, PiT1 and PiT2 P_i transport is impaired, yet sufficient. PiT1 and PiT2 transport was ~54% and ~58% of the transport in the absence of both divalent cations, respectively. Neither SLC20 protein is strictly dependent on Ca^{2+} and/or Mg^{2+}, but studies have indicated that Mg^{2+} is dispensable as long as Ca^{2+} is present. Ca^{2+} involvement increased P_i transport the greatest, indicating that Ca^{2+} may have a regulatory function. PiT1 is the only SLC20 paralog that can substitute Mg^{2+}, albeit only partially, in the absence of Ca^{2+}.

PiT1 and PiT2 transporters are highly related, but there are a few differences. A notable functional difference is that PiT2 is the only isoform that can mediate Na^+-independent Pi transport by translocating H^+ (3).

There are no known inhibitors of SLC20 family proteins. In contrast, NaPi-II proteins are inhibited by PFA. Although there are reports that PFA inhibits PiT proteins, the PFA concentration was high (>10 mM) and the membrane potential was not controlled, indicating that the inhibition might be nonspecific. Although there are no inhibitors of PiT2, arsenate does compete with P_i to reduce P_i transport in PiT proteins. These effects are similar in NaPi protein isoforms (33).

SLC20 and SLC34 in a Physiological System

The unrelated SLC20 and SLC34 families are unique because of their specificity for one of two phosphate species at physiological pH. Distinguishing characteristics of each family and its paralogs are displayed in Table 1. It is unclear whether these functional differences have any impact on the proteins' physiological purposes. It should be noted that transporting either of the phosphate species will change the pH due to the equilibrium shift. The two solute carrier families differ in their optimum pH range but have an overlapping pH of 6.8. The PiT proteins have the greatest transport rate in the acidic range whereas the NaPi proteins favor transport in the alkaline range. Interestingly, the difference in substrate stoichiometry and preferred P_i species creates a 100-fold difference in P_i concentrative capacity. The difference in substrate stoichiometry may have physiological implications. NaPi-IIc transports one less Na^+ ion and is electroneutral. Thus, NaPi-IIc-mediated transport has a smaller energetic cost because less Na^+ is loaded into the cell and less energy is needed to keep the cell at a negative membrane potential

(33). PiT-type transporters could be favorable in the CNS because both PiT proteins respond to variations in extracellular P_i concentrations and a persistent deficiency will increase PiT1 and PiT2 mRNA. On the other hand, NaPi-II-type transporters are more sensitive to dietary P_i intake and hormonal factors.

1.4 Phosphate Transport in Other Tissues

To better understand phosphate transport in the CP, it is useful to first consider phosphate transport in other tissues. The kidneys and the small intestines are two sites that are important in the maintenance of systemic P_i homeostasis and a brief review of phosphate balance in each organ is given below.

Renal Phosphate Transport

The major site of P_i maintenance resides in the kidneys, primarily in the proximal tubules. The human kidneys are responsible for the reabsorption of 80% of the free phosphate ions that are filtered by the glomeruli with approximately 60% to 70% reabsorbed in the proximal tubules and 10 to 20% in the distal sites (17). The principle and rate-limiting step in P_i reabsorption is mediated by sodium-dependent P_i transporters that are in the brush border membrane. NaPi-II-type and PiT-type transporters are both present in the kidney, with the former as the central transporter (17, 18, 27) (Figure 5). The brush border membrane has both NaPi-IIa and NaPi-IIc isoform, and NaPi-IIa knockout mice have designated this isoform as the major player in systemic P_i homeostasis. This was supported by the 70% reduction in sodium-dependent P_i cotransport in the apical membrane in NaPi-IIa knockout mice. The NaPi-IIc type KO mice model demonstrated that the type IIc transporter accounts for 30% of renal Na/P_i

mediated transport in the brush border membrane. PiT1 and PiT2 mRNA have been detected in proximal tubular cells but their protein localization has yet to be determined (17). Figure 5 is a schematic of the P_i transport in renal cells.

Intestinal Phosphate Transport

The U.S Department of Agriculture's Continuing Survey of Food Intakes by Individuals suggests a daily phosphorus intake in the range of 1,600 to 2,400 milligrams for males and 1,200 to 1,600 milligrams for females. Fortunately, phosphorus is abundant in almost all food types and is ingested as P_i. Phosphates in the diet exist first as organic molecules that must be broken down by digestive enzymes to release P_i into intestinal fluids. The freed P_i is then ready for absorption by the intestine (9).

The primary site of P_i absorption is along the entire length of the small intestine, with some absorption at the colon when intestinal luminal P_i concentrations are extremely high. In vitro studies involving voltage clamp analysis or radiolabeled uptake have proven the existence of an active sodium-dependent P_i transport pathway in intestinal cells..

The active transport of P_i is mediated by NaPi-II-type transporters and PiT-type transporters. Unlike the kidney, the small intestines employ the NaPi-IIb isoform for sodium-dependent, inward transport of extracellular P_i. NaPi-IIb-type transporters have a relative high affinity for P_i (K_m 10 μM), which suggests that NaPi-IIb can be saturated under most dietary conditions and is effective at transporting P_i even under conditions of dietary phosphate depletion. NaPi-IIb knockout studies have been performed in mice, and although decreased intestine phosphorus absorption has been reported in the KO mice, serum phosphorus and calcium concentrations were kept constant (25). This phenomenon may be explained by

compensatory mechanisms by the renal NaPi-IIa-type transporter and suggests that NaPi-IIb may be involved in the regulation of systemic P_i levels.

Approximately 10% of the sodium-dependent P_i transport is not attributable to NaPi-IIb-type transporters, resulting in the search for other P_i transporters in the small intestine. Although PiT proteins have been found in the basolateral membrane in a variety of tissues, evidence has demonstrated that PiT1 protein and PiT2 protein are actually expressed on the apical side of enterocyte epithelium. Literature has shown that NaPi-IIb-type and PiT-1-type transporters are primarily expressed in the duodenum and jejunum of rat small intestine (25). The role of PiT transporters in the small intestines has yet to be determined.

1.5 Radiolabeled Phosphate Uptake Studies in Rat Z310 Choroid Plexus Epithelial Line

The present study is based on the observations of radiolabeled phosphate uptake by rat Z310 choroid plexus epithelial cells (Bataille et. al. (Unpublished)). The study showed that radiolabeled P_i uptake by Z310 cells increased as a function of time (Figure 6) and was not saturated at normal CSF P_i concentrations (0.9 mM) (Figure 7A). The Eadie-Hofstee plot (Figure 7B) was generated by studying the transport of P_i by the Z310 cells at increasing external P_i concentration and indicated a K_m=0.56 mM and V_{max}= 7.68 nmoles/mg protein/5 minutes. Furthermore, Bataille et al. (unpublished) conducted studies which suggested that the primary P_i transporter is electrogenic and Na^+ dependent, but can substitute Na^+ with Li^+ (Figure 8). This was evident by the inhibition of P_i uptake in the absence of sodium and by plasma membrane depolarization induced by high potassium Ringer and a diminished sodium gradient created by inhibiting Na^+/K^+/ATPase by 1 mM ouabain. Additionally, transporter inhibition studies were performed, and reduced P_i transport was observed in the presence of arsenate and antimycin A

when compared to the control. There was no change in transport when the Z310 cells were incubated with phosphonoformic acid (PFA) or methazolamide. (Figure 9).

The uptake studies conducted by Bataille et al. (unpublished) described P_i uptake in Z310 choroid plexus cells as sodium-dependent, able to partially substitute Na^+ with Li^+, electrogenic, and inhibited by arsenate but not PFA. Based on Table 1(33), the P_i uptake properties are consistent with those of PiT-like transporters. In addition, Bataille et. al. performed PiT2 localization studies in Z310 CP cells (Figure 10) that show that PiT2 protein is present and appears to be localized to the plasma membrane.

1.6 The Present Study

The cerebrospinal fluid provides the optimal environment for neurons to properly function. Interestingly, CSF P_i concentrations are one-half that of blood plasma. Thus, we questioned why the brain parenchyma prefers a lower P_i concentration than its plasma counterpart. We sought to determine the primary mechanism of P_i transport from the cerebrospinal fluid to plasma. Bataille, et al. (unpublished) conducted extensive radiolabeled uptake P_i in Z310 CP epithelial cells that suggest that the PiT family is the principle pathway for P_i to exit the CSF. This was based on electrogenic and sodium-dependent P_i transport along with partial transport when Na^+ was substituted with Li^+ and inhibition by arsenate but not PFA. However, it remained to be determined whether NaPi-II-type transporters are present or absent in the CP. Therefore, the present study examined the presence of NaPi-II type family in CP secondary-active P_i transport in rat choroid plexus epithelial cells. To do this, semi-quantitative RT-PCR and western blotting studies were performed to determine if NaPi-II mRNA and protein

are expressed. Our results indicate that NaPi-IIb-type transporters may be in the rat choroid plexus, along with PiT1 and PiT2 transporters.

2. MATERIALS AND METHODS

2.1 Animal and Tissue Preparation

Intact rat choroid plexus, renal proximal tubule, gut, and lung tissues were from Sprague Dawley rats of mixed gender and varying ages and weight. Tissues were stored in RNAlater RNA stabilization reagent (Qiagen). The adult rat choroid plexus epithelium tissues in primary culture were from the lateral ventricle and were provided by Dr. Alice Villalobos. All tissues were stored at -20°C and thawed on ice prior to use.

2.2 Reverse Transcriptase-Polymerase Chain Reaction (RT-PCR) and PCR Product Visualization

RT-PCR analysis was conducted on adult and neonate rats for semi-quantitative mRNA analysis of NaPi-II-type and PiT-type transporters. Total RNA was extracted from adult and neonate rat choroid plexus cells, rat renal proximal tubule cells, rat gut cells, and rat lung cells using a Qiagen RNeasy mini kit. A Thermo Scientific Nanodrop was used to measure RNA concentrations. Twenty-five microliter RT-PCR master mixes were prepared using a Qiagen OneStep RT-PCR kit. 1 µg of total RNA of each sample was added to each master mix, which had a final reverse and forward primer concentration of 0.6 µM. The primers were designed against rat NaPi-IIa (SLC34A1, Accession # NM_013030.1, 630 BP), rat NaPi-IIb (SLC34A2, Accession #NM_053380.2, 856 BP), rat NaPi-IIc (SLC34A3, NM_139338.1, Set 1 513 BP, Set 4 786), rat PiT1 (SLC20A1, Accession # NM_031148.1, 758 BP) and rat PiT2 (SLC20A2,

Accession # NM_017223.2, 337 BP). Table 2 shows the nucleotide sequence, the nucleotide correspondence, and the amplified fragment size of each primer.

RT-PCR was conducted in a PCR Sprint thermocycler (Thermo Electron Corporation). PCR amplification begins with an initial heating step at 50°C for thirty minutes and then 95°C for fifteen minutes to activate the HotStarTaq DNA polymerase. The cycle parameters are as follows: 94°C denaturing for 1 minute, 56°C annealing for 1 minute, and 72° extension for 1 minute. The thermocycler was programmed for 32 cycles. Final extension was at 72°C for ten minutes and then held at 4°C until products were removed from the thermocycler.

PCR products were visualized on a 1% agrose gel with 0.1% of GelStar (nucleic acid stain). Fifteen microliters of the samples were loaded with 3 µL of 6X loading buffer (glycerol, 0.5 M EDTA pH 8.0, 1% bromophenol blue). The gel was run at 70 V for approximately 3 hours. A 1 KB plus DNA ladder (Invitrogen) was loaded and a UV detector was used to visualize the bands.

2.3 Western Blotting

PiT1, PiT2, and NaPi-IIb protein expression was analyzed by western blotting. Intact rat choroid plexus cells were vigorously vortexed with 250 µL distilled H_2O, 2.5 µL 1M KOH, and 5 µL 2% protease inhibitor cocktail and then centrifuged at maximum speed for 1 minute. The supernatant was measured for protein concentration by Bio-Rad protein assay and then diluted 2X with Kaman buffer. The samples were not boiled prior to electrophoresis. Proteins were separated by SDS-polyacrylamide gel electrophoresis at 120 V for 3 hours. The resolving and stacking gel was 10-12% and 4% acrylamide, respectively. Approximately 40 µg of each sample was loaded into each lane. A 5 µL full range rainbow MW marker (GE Healthcare) was also

loaded to measure protein size. Proteins were transferred to a polyvinylidene difluoride membrane using a transfer buffer (25 mM tris base, 192 mM glycine, 10% MeOH, 0.01% SDS, pH 8.3) and blocked with 3% PBS/tween/milk. The blot was probed with primary antibody in 3% PBS/tween/milk (PiT1, PiT2, NaPi-IIb 1:500 dilution; β-actin 1:500 dilution). The membrane was incubated with PiT2, PiT1, and NaPi-IIb primary antibody overnight whereas β-actin antibody was incubated with the membrane for 2 hours. Secondary antibody conjugated to horseradish peroxidase (HRP) was then added for approximately 1 hour. ECL western blotting reagent (Pierce) was used for band detection and exposed on ECL hyperfilm.

Rabbit NaPi-IIb antibody (Accession # Q9DBP0) was from Abbiotec Company, San Diego, CA, rabbit anti-PiT1 (74 kDa) was obtained from Santa Cruz Biotechnology, Inc., and Dr. Victor Sorribas of the Universidad de Zaragoza provided us with the rabbit anti-PiT2. The secondary antibody was a goat anti-rabbit conjugated to horseradish peroxidase (Sigma Aldrich). The anti-β-actin was from Sigma-Aldrich.

3. RESULTS

3.1 Results of RT-PCR of Adult and Neonate Rat Choroid Plexus

RT-PCR was performed to determine the presence or absence of SLC34 and SLC20 mRNA in adult and neonate rat choroid plexus cells. To ensure that the SLC34 and SLC20 primers were properly functioning, negative and positive control RT-PCR analyses were conducted. Several sources have confirmed the presence of NaPi-IIa and NaPi-IIc but not NaPi-IIb in the kidney (17, 18, 33). In contrast, the intact rat gut tissue has been reported to exclusively express the NaPi-IIb isoform (18, 25, 33). Figure 11A and 11B show the results of the RT-PCR of intact rat renal proximal tubule tissue and intact rat gut tissue. The RT-PCR confirmed the

presence of NaPi-IIa (~630 bp) and NaPi-IIc ((1) ~513 bp, (2) ~786 bp) in the rat renal proximal tubule; however, there was also a signal for NaPi-IIb (~856 bp). Since the proximal tubule tissue used in this analysis was intact, there was more than just nephron tissue in each sample. The extraneous tissue could be blood cells, endothelial cells or smooth muscle tissue that could account for the NaPi-IIb mRNA signal. The RT-PCR of the rat gut cells showed a signal for the NaPi-IIb isoform but not for NaPi-IIa and NaPi-IIc mRNA. This is consistent with the literature and further confirms the functionality of the primers.

After testing the integrity of the primers, RT-PCR analysis was conducted on intact rat choroid plexus tissues to determine the presence of any NaPi-II isoform. The results are displayed in Figure 13 with rat kidney used as the control. There were no bands detected for any of the NaPi-II isoforms in rat CP but strong signals for NaPi-IIa (~630 bp) and NaPi-IIc (~786) and a weak signal for NaPi-IIb in the kidney tissue (~856 bp).

Additionally, a RT-PCR was performed on intact adult rat CP using PiT1 (~758 bp), PiT2 (~337 bp), and NaPi-IIb (~856 bp) primers. The results are shown in Figure 12A. There was no PiT1 mRNA detection but there was a strong signal for PiT2 and a weaker signal for NaPi-IIb. A repeat of the preceding analysis was performed, but we used isolated choroid plexus epithelium in primary culture of adult and neonate rats as our samples. Figure 12B shows the results of the RT-PCR, which show a signal for both PiT1 and PiT2, albeit PiT2 had a stronger signal. No NaPi-IIb mRNA was detected in adult and neonate rat samples. Thus, it is not definitive whether NaPi-IIb mRNA is present in rat choroid plexus epithelium.

3.2 Results of Primary Rat Choroid Plexus Western Blot

The results from the RT-PCR have excluded the presence of NaPi-IIa and NaPi-IIc mRNA in the rat CP but confirmed the presence of PiT2 mRNA in the CP. The RT-PCR data on PiT1 and NaPi-IIb mRNA was inconclusive and a western blot was performed to determine protein expression. A western blot was also done to confirm PiT2 protein expression. Intact human choroid plexus tissues were analyzed alongside intact rat CP. The results are revealed in Figures 14 (PiT1 Expression), Figure 15 (PiT2 Expression), and Figure 16 (NaPi-IIb Expression). PiT1 expression was established in the rat and human CP by the presence of a band at ~74 kDa. Additionally, the immunoblot revealed the presence of PiT2 protein in rat and human CP by a band at ~72 kDa. The PiT2 western blot also showed bands present at ~76 kDa, and ~140 kDa that can be explained by glycosylation and dimerization, respectively (26, 33). The NaPi-IIb immunoblot indicated that NaPi-IIb proteins are expressed in the human and rat CP by the presence of a ~108 kDa band. Rat lung, which has been confirmed to only have NaPi-IIb-type transporters, was used as a positive control (8). Each immunoblot also included assay of β-actin (~42 kDa) to ensure equal protein loading between each sample. In the rat lung sample, the β-actin sample showed three bands. This is because of cell apoptosis which results in cleavage products. The initial cleavage results in a band at 41 kDa that appears as a doublet and further cleavage gives a major band at 30 kDa. The cleavage products could be a result of the actions of interleukin 1β-converting enzyme (1, 11).

4. DISCUSSION

This study attempted to address how P_i is actively transported out of the CSF. The Bataille et al. radiolabeled P_i uptake studies suggested that P_i transport has PiT-like characteristics. However, it has not been determined whether NaPi-II-type transporters play a role in mediating P_i transport. Figure 12A and Figure 12B display the results of an RT-PCR of rat CP and suggest the presence of PiT1, PiT2, and NaPi-IIb mRNA in the CP. The RT-PCR in Figure 12A showed that neonate and adult rat CP have PiT1 and PiT2 mRNA, with a stronger signal for PiT2 mRNA. Another sample of adult rat CP was also analyzed by RT-PCR with the same three primers and was revealed to have NaPi-IIb mRNA and PiT2 mRNA expression. Although PiT2 was found in all three samples, PiT1 and NaPi-IIb mRNA expression in the rat CP samples were inconsistent. This may be explained by the difference in sample preparation in Figure 12A and Figure 12B. In Figure 12A, the rat CP samples were isolated rat choroid plexus epithelium in primary culture whereas the samples in Figure 12B were intact rat choroid plexus tissue. The intact rat choroid plexus tissue has more than just CP epithelium. The choroid plexuses are leaf-like structures with rich capillary beds that are attached to the ependyma by a thin stalk. Additionally, the CP is lined with the ependyma to form its outer covering (23). Therefore, intact rat CP could include endothelial cells, smooth muscle, blood cells, and ependymal tissue that may have NaPi-IIb-type transporters.

In addition, Lau et al. reported PiT1- and PiT2-type transporters expression in rat vascular smooth muscle cells, with PiT1-type transporters more abundant than PiT2-type transporters. No NaPi-II isoform expression was seen (12, 30). Moreover, Di Marco et al. studied hyperphosphatemia, phosphate transport, and endothelial cell apoptosis. The investigators found PiT1 mRNA in endothelial cells but have not ruled out the presence of other P_i transporters. The

investigators also found that PFA prevented phosphate-induced apoptosis, suggesting that NaPi-II transporters may be present in endothelial cells (14). Thus, tissue contamination could account for the PiT1 and NaPi-IIb signal.

This type of contamination can be seen in our control samples. In Figures 11 and Figure 13, the rat kidney was used as a control to ensure the specificity of NaPi-II primers. According to Murer, et al, renal proximal tubules only contain NaPi-IIa- and NaPi-IIc-type transporters, which was confirmed in the RT-PCR; however, we detected a signal for NaPi-IIb, which has been reported to be absent from the nephron (18). The intact rat kidney tissue included not just proximal tubule but endothelial cells, blood cells, and smooth muscle cells. Thus, this may be an example of contamination that could cause a false-positive for NaPi-IIb and explain the NaPi-IIb signal in the rat CP samples.

In addition to RT-PCR analysis, western blot analysis of PiT1, PiT2, and NaPi-IIb was performed to determine protein expression. The immunoblots indicated that intact rat CP have PiT1, PiT2, and NaPi-IIb proteins. Moreover, intact human CP samples were analyzed for protein expression and suggest the presence of PiT1, PiT2, and NaPi-IIb transporters. Because intact CP tissues were used, samples contained other tissues besides CP epithelium tissues that could account for the band in the immunoblot.

The contamination of CP with non-target tissues has been problematic in our study. Although it is likely that PiT2-type transporters are the principle transporter in the CP, we cannot rule out PiT1 and NaPi-IIb. Thus, we must do immunohistochemistry studies to determine the localization of these transporters.

P_i Cellular Homeostasis and CP Function

Although the results suggest that NaPi-IIb could possibly play a role in CP P_i transport, PiT2-type transporters seem to have a definite role in P_i transport out of the CSF. This has been suggested by the PiT-like P_i uptake, PiT2 mRNA and protein expression, and the apparent PiT2 localization in the plasma membrane of Z310 CP cells. These observations raise the question of why choroid plexus cells have PiT-type transporters instead of NaPi-II-type transporters. NaPi-II transporters are primarily expressed in the kidney and the gut, which reflects the SLC34 family's principle role as the regulator of systemic P_i homeostasis. In contrast, because PiT-like transporters have wide tissue distribution, it has been suggested that they function as a regulator of cellular P_i homeostasis. PiT-1-like and PiT-2-like transporters have been found in all investigated human tissues, although at different levels. Moreover, PiT mRNA is regulated by various factors that include epinephrine, platelet-derived growth factor (PDGF), insulin-like growth factor (IGF-1), and most importantly, P_i concentrations (33). Reports have shown that persistent P_i starvation increases PiT1 and PiT2 mRNA. Interestingly, the [P_i] regulation of PiT-2 transporters results in the formation of PiT-2 dimers, suggesting that PiT2 proteins play a role in phosphate sensing. Phosphate uptake is 4.5 and 2.5 times more efficient in phosphate deprived conditions than at 10 mM. In addition, PiT2 activity changes within minutes of P_i concentration variations. The adaption to P_i concentrations occurs without any significant modification to the number of PiT2 proteins, but rather a change in PiT2 structure, as seen in Figure 17. Salaün et al. reported that PiT2 assemblies, particularly those at the cell surface, may switch between two conformations. The proportion of individual PiT2 molecules that can be cross-linked is high in low extracellular P_i concentrations but is low in high extracellular P_i concentrations. Moreover, human PiT2 has positive cooperativity characteristics that are reflected by the dimerization of

human PiT2 in P_i starved environments (26). The ability of PiT-type transporters to finely sense extracellular P_i concentrations and quickly adapt to extracellular P_i concentrations is favorable for maintaining the CSF environment.

The P_i sensitivity of PiT-type transporters is essential if the primary function of the brain choroid plexus is taken into account. The ability to mediate the transport of solutes and produce cerebrospinal fluid is an energetically expensive process. Thus, the choroid plexus contains a high volume of mitochondria to support CSF secretion and maintain ionic gradients. In fact, Cornford, et al. reported a high mitochondrial volume (>13% of cytoplasmic volume) in mammalian choroid plexus cells that exceeds any previously reported brain cell (5). P_i plays a major role as a structural component of ATP and its uptake into the CP is essential for its function. If PiT-transporters are responsible for cellular P_i homeostasis, then its sensitivity to P_i is more optimal for providing enough ATP for CP function.

CSF pH and PiT-Type Transporters

One of the most interesting, unexplained phenomenons of the CNS is the ability of the CSF to maintain a constant pH in the absence of protein. Because of the lack of protein, it seems likely that the CSF contains a large buffer concentration, particularly P_i, a dominant physiological buffer. However, CSF P_i concentrations are held between 0.5 and 1.0 mM, about one-half the P_i concentration of the plasma (2). This low CSF P_i concentration is unexplained but may still play a role in the maintenance of CSF pH. A major difference between the SLC20 and SLC34 transporter gene families is their optimal pH range and preferred P_i substrate. The PiT proteins favor transport in the acidic range, and because PiT-type transporters favor $H_2PO_4^-$, PiT-mediated P_i transport would alkalinize the CSF. However, the most notable characteristic of PiT2

transporter is the ability to co-transport P_i with H^+, unlike the NaPi-II-type transporters. Thus, PiT-mediated transport may be optimal because it can operate at low pH and at the same time alkalize the CSF. In fact, PiT2 is the only sodium-dependent P_i transporter that can undergo Na^+-independent-P_i transport by translocating H^+.

Central Control of Phosphate Appetite in Rats and Role of PiT-Type Transporters

The lack of any essential nutrient in the diet has physiological implications. For example, zinc, magnesium, and potassium deficiency disrupt body growth and affect food intake variation. A disturbance in P_i homeostasis has serious repercussions, including bone abnormalities, stunted growth, and metabolic disorders. Typically, mineral deficiencies cause an increase in Na^+ ingestion; however, this is not the case with P_i, suggesting that P_i appetite is specific to P_i concentrations. Several groups have reported that dietary P_i has a direct effect on P_i craving. In 2007, Ohnishi et al. performed a study that investigated whether a lowered Pi concentration in plasma and CSF will induce a P_i appetite in rats. The results showed that rats that were under a low P_i diet consumed 70%-100% more P_i than normal P_i diet rats. Moreover, low P_i diet rats had a significant reduction in P_i concentrations in the CSF and plasma (20). These results demonstrate that P_i appetite can be induced in rats and suggest that its action is through lowered plasma and CSF P_i concentrations.

The Ohnishi et al. study indicates that there is some central control that regulates P_i concentrations. However, it is unknown how the body manages to sense low P_i concentrations. The PiT-type family could potentially explain this phenomenon if it is present in the apical membrane of choroid plexus cells. As seen in Figure 17, PiT-type transporters adapt a

conformation that reflects the presence of a low or high P_i concentration and could potentially act as the P_i sensor in CSF (26).

PiT2-Type Transporters, Calcium, and Inhibitors

The SLC20 family of transporters is also distinguished by the modulatory effects of divalent ions. PiT1- and PiT2-type transporters exhibited impaired, albeit sufficient, P_i transport in the absence of Ca^{2+} and Mg^{2+}. Of the two divalent ions, Ca^{2+} increased P_i transport more significantly, suggesting that Ca^{2+} may regulate PiT function (3). The role of Ca^{2+} in CP P_i transport is noteworthy because of the concerted homeostasis of calcium and phosphate. As previously discussed, hypocalcemia increases neuronal permeability to Na^+ which can result in CNS hyperexcitability whereas hypercalcemia can cause CNS depression. Thus, the unique ability of PiT-type transporters to be modulated by Ca^{2+} could be beneficial to maintaining an optimal milieu for the CNS.

The last major advantage of the PiT family is its lack of reported inhibitors, unlike the NaPi-II family, which is reported to be inhibited by PFA (33). This is a major benefit that ensures that the CP and CSF obtain sufficient amounts of P_i.

5. CONCLUSIONS

The present study focused on P_i transport out of the CSF and into CP cells. Although more studies need to be performed to determine the mechanism of CP P_i transport, it is likely that PiT2-type transporters play the largest role in mediating P_i out of the CSF, with a smaller contribution from PiT1-type transporters. Although Bataille et al. reported PiT-like P_i uptake, NaPi-IIb-type transporters may contribute to CP P_i transport. Figure 18 is a proposed model for CP P_i transport. The apical membrane may have PiT1, PiT2, and/or NaPi-IIb but all transport is electrogenic, bringing in a net positive charge. PiT-mediated transport introduces a positive charge, along with a build-up of $H_2PO_4^-$ and Na^+. To prevent the accumulation of $H_2PO_4^-$ and a positive potential, there must be a transporter at the basolateral membrane that pushes $H_2PO_4^-$ out of the CP cell. The removal of $H_2PO_4^-$ alkalizes the cell while also removing a net negative charge. A potential basolateral transporter that is capable of balancing the removal of H_2PO_4 is the Cl^-/HCO_3^- exchanger, AE2. This transporter has been reported to be localized exclusively to the basolateral membrane of the mammalian CP and is known as a Cl^- loader and base extruder (7). Thus, the acidic H_2PO_4 is pushed out of the CP with the basic HCO_3^-. Moreover, a sodium gradient must be sustained to continue to the uptake of P_i.

More work needs to be performed to perfect the CP P_i transport model. However, the significance of this study is that we now know that NaPi-IIa and NaPi-IIc transporters are not present in the choroid plexus. Determining the mode of CP P_i transport is important because physiological impact of P_i. Future work in CP P_i may help us clinically by explaining such phenomena as CSF formation or acid-base balance that when deregulated cause such pathologies as congenital hydrocephalus or CNS acidosis.

6. AKNOWLEDGEMENTS

I would like to extend many thanks to Dr. Larry Renfro, my research, university scholar, and honors advisor, who supported and guided me throughout this whole project. Many thanks are also extended to Dr. Amy Bataille for her collaboration on this project and Sonda Parker, whose technical skills and support made this experience possible. Moreover, I would like to thank Dr. Joseph Crivello and Dr. Amy Howell, who were both on my University Scholar committee, and the University of Connecticut University Scholar and Honors Program. Finally, thank you to Dr. Victor Sorribas for providing us with the PiT2 antibody and Dr. Villalobos for providing us with primary rat choroid plexus epithelium.

This manuscript was supported by the National Science Foundation.

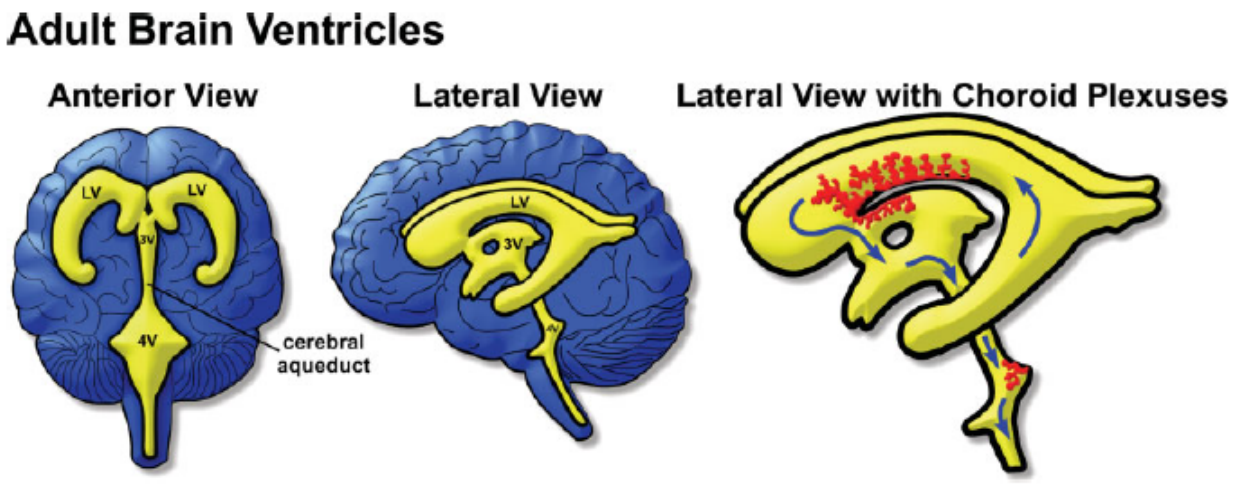

FIGURE 1. Cartoon Representation of Adult Human Brain Ventricles by Lowry et. al. Blue is brain tissue, yellow is the brain ventricles, and red is the choroid plexuses. The blue arrows show the direction of CSF flow. LV= Lateral Ventricle, 3V= Third Ventricle, 4V=Fourth Ventricle

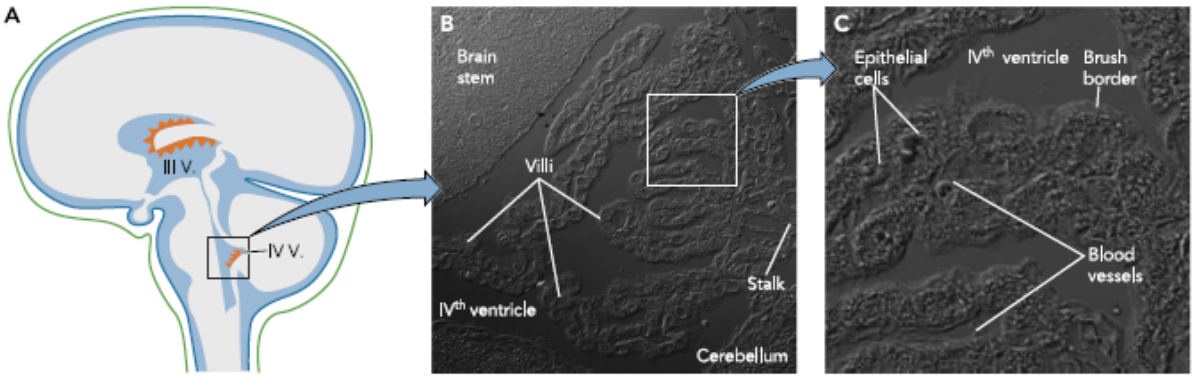

FIGURE 2.Schematic Representation and Differential Interference Contrast Micrograms of Mouse Choroid Plexus by Damkier et. al. (A) Schematic representation of the brain and its ventricular system. Choroid Plexus is in orange, cerebrospinal fluid is in light blue, brain parenchyma is in gray, meninges in dark blue, and skull in green. III V. is the third ventricle and IV V is the fourth ventricle. (B) Differential interference contrast micrograph of the mouse fourth ventricle and choroid plexus at low magnification. (C) Higher magnification of a single villus of the same choroid plexus.

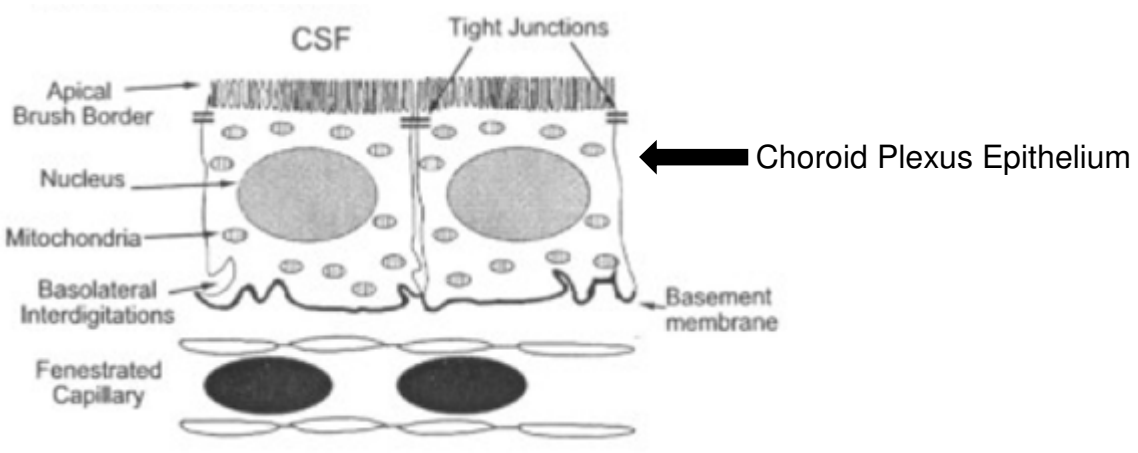

FIGURE 3. Morphology of Blood-CSF Interface by Johanson et. al. The choroid plexus is a monolayer of cicumferentially arranged epithelial cells with a fenestrated capillar at its center and contains numberous mitochondria. The CP capillaries, unlike other brain caplicaries, are permeable to macromolecules.

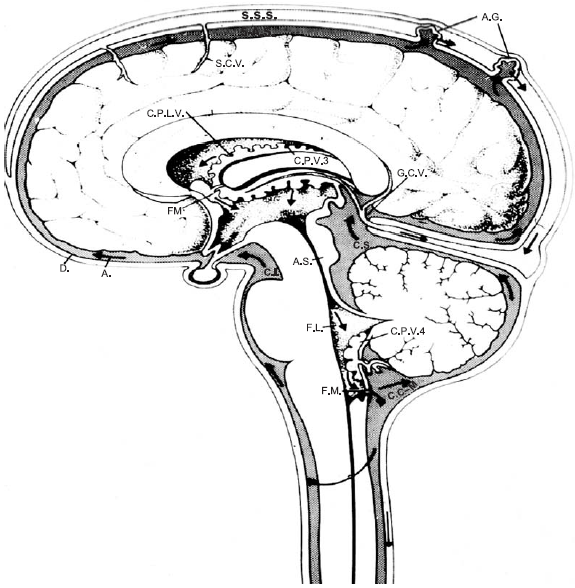

FIGURE 4. A Schematic Section through the Brain and Spinal Cord Showing the Drainage Pathways for CSF. CSF is formed by the choroid plexuses of the lateral ventricle (CPLV) and passes by the two foramina of Munro (FM) into the third ventricle (CPV3), where more CSF is produced by the CP. CSF then flows through the aqueduct of Sylvius (AS) and into the fourth ventricle. The CSF exits into the various basal cisterns (CI, CS) and then into the subarachnoid space (SAS) through the paired foramina of Luschka (FL) and single foramen of Magendie (FM). CSF flows through the subarachnoid space over the surface of the cortex. Some fluid drains into the blood via the arachnoid granulation (AG) into the superior sagittal sinus (SSS).

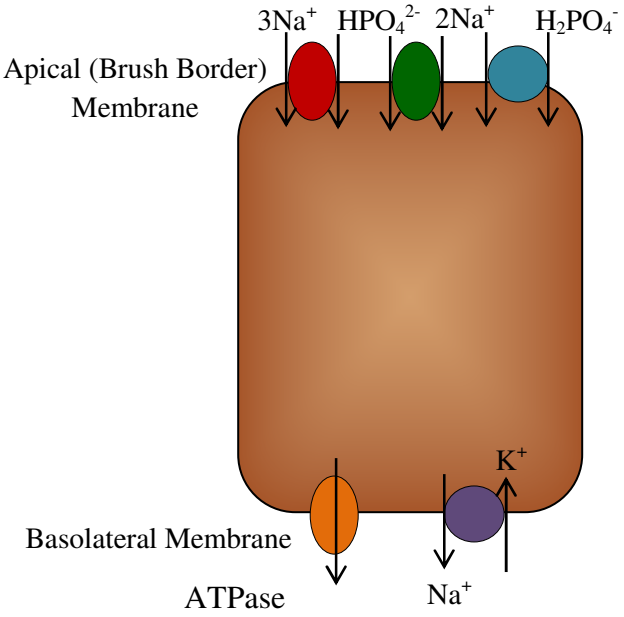

FIGURE 5. Localizations and Substrates of Sodium-Dependent P_i-Type Transporters in the Kidney. The brush border membrane has NaPi-IIa (Red), NaPi-IIc (Green), and PiT2 (Blue) transporters, whereas the basolateral membrane has Na^+-K^+-ATPase (Purple) and an unknown transporter (Orange) that mediates the movement of P_i back into the blood plasma.

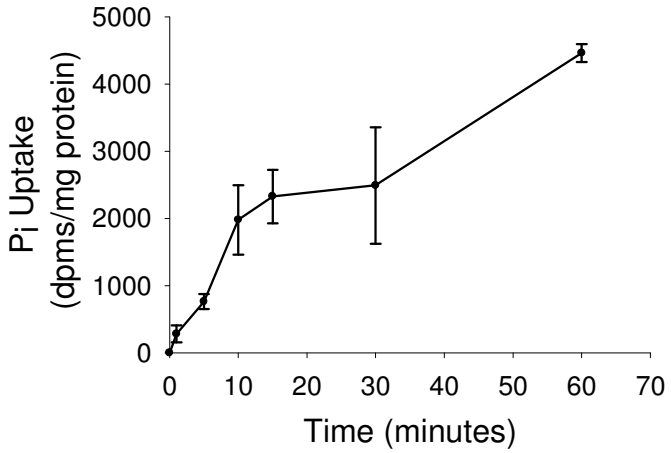

FIGURE 6. Summary Data-P_i Uptake in Z310 Rat CP Epithelial Cell Line as a Function of Time. P_i uptake was determined by the amount of radiolabeled P_i inside the cells at different time intervals. The amount of P_i inside the cell was normalized by the protein concentration of each sample. The figure demonstrates that uptake is linear at t= 5 minutes and is used as time frame for the other uptake experiments.

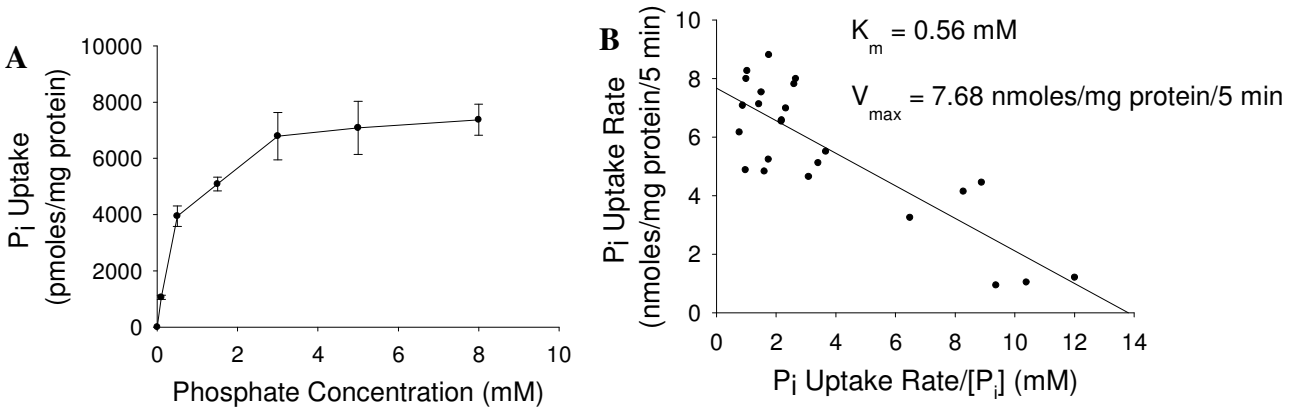

FIGURE 7. (A) Summary data of the P_i uptake in Z310 rat CP epithelial cell line at different external P_i concentrations. Uptake was determined by the amount of radiolabeled P_i inside the cells at t= 5 minutes and was normalized by the protein concentration of each sample. The results show that P_i uptake is not saturated at physiological P_i concentration (0.9 mM). **(B)** A Eadie-Hostee plot was created from the summary data and revealed that P_i uptake has a K_m of 0.56 mM and V_{max} of 7.68 nmoles/mg protein/5 minutes.

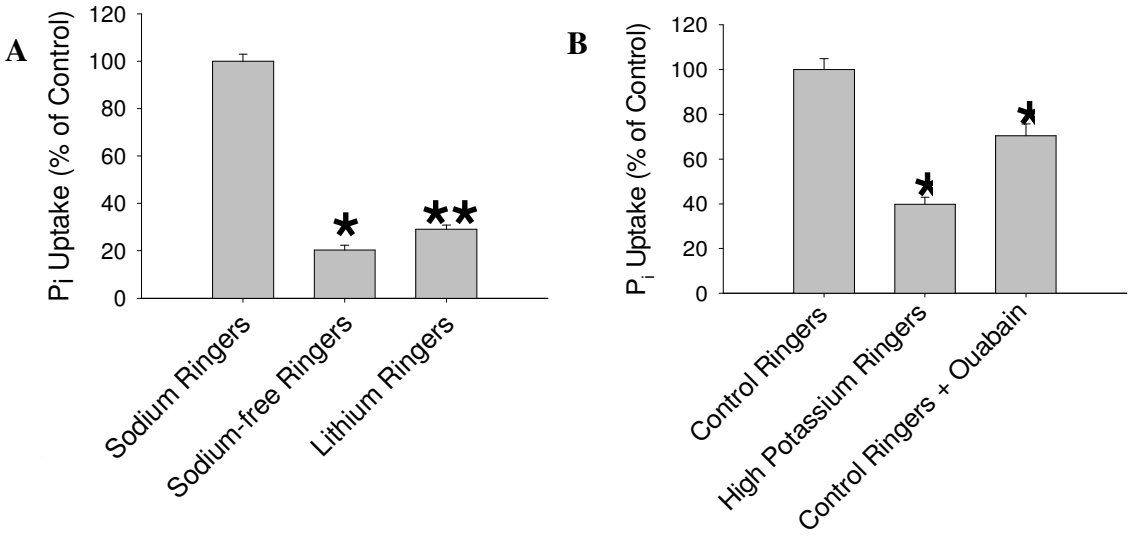

FIGURE 8. Summary Data of P_i Uptake in Z310 Rat CP Epithelial Cell Line in the Presence and Absence of Several Ions and Gradients. CP cells were pre-incubated in their respective treatments for 30 minutes before radiolabeled P_i was added at t=0 minutes. Uptake was then determined by measuring the amount of radiolabeled P_i inside the cells at t=5 minutes and normalizing the amount by the protein concentration of each sample. **(A)** P_i uptake is inhibited when NaCl is removed from the medium (sodium-free ringers). However, uptake was partially restored when 120 mM LiCl (lithium ringers) was added. **(B)** P_i uptake is inhibited by plasma membrane depolarization that was induced by high potassium Ringer (100 mM KCl) and by a diminished sodium gradient. The diminished sodium gradient was created by inhibiting the Na^+/K^+/ATPase by 1 mM ouabain.
*Significantly different from the control or sodium ringers
** Significantly different from sodium-free ringers

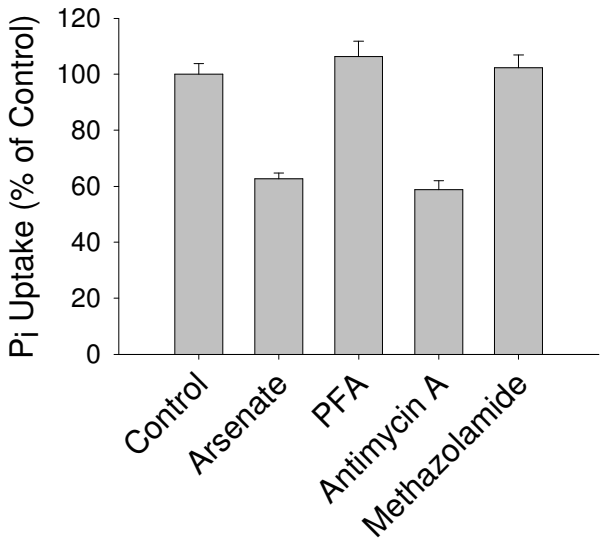

FIGURE 9. Summary Data of P_i Uptake in Z310 Rat CP Cell Line in the Presence of Various Known Phosphate Transporter Inhibitors Cells were pre-incubated in their respective inhibitor treatments for 30 minutes before radiolabeled P_i was added at t=0 minutes. P_i uptake was determined by the amount of radiolabeled P_i inside the cells at t= 5 minutes and was normalized by the protein concentration of each sample. Arsenate (10 mM) and antimycin A (0.1 mM) inhibited P_i uptake when compared to controls. There was no change in P_i uptake when the cells were incubated with 1 mM PFA or 0.1 mM methazolamide.

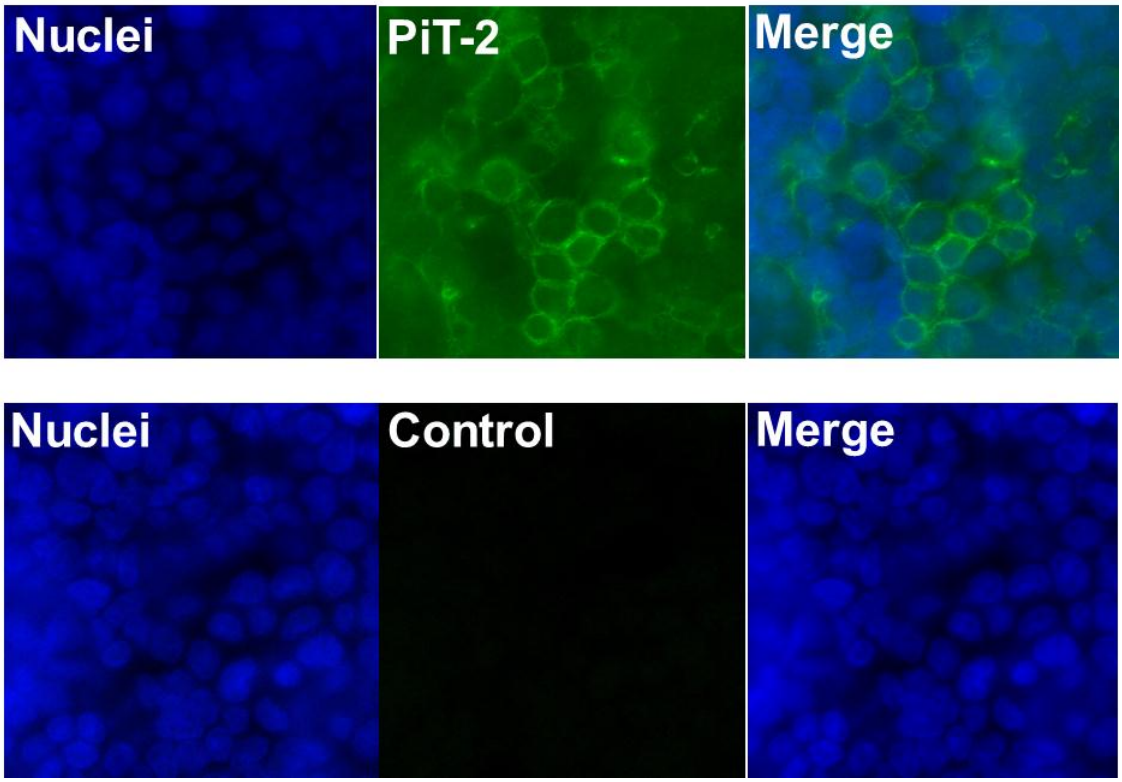

FIGURE 10. Fluorescence Immunohistochemistry Analysis of PiT2 Protein Expression in the Z310 Choroid Plexus Epithelial Cell Line. PiT2 staining was done with a commercially available anti-PiT2 (Sigma Aldrich) and a fluorescently tagged secondary antibody (green). Controls were labeled with secondary antibody only. The nuclei were visualized with Hoesct stain (blue).

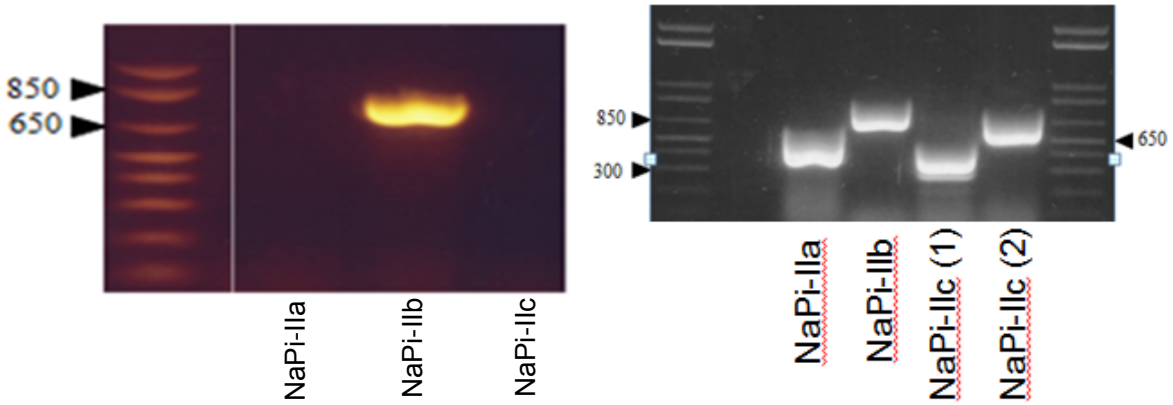

FIGURE 11. Semi-Quantitative RT-PCR Products of mRNA Extracted from Rat Kidney and Rat Gut. Primers were designed against the rat mRNA sequences for NaPi-IIa (SLC34A1, accession # NM_013030.1, 630 bp), NaPi-IIb (SLC34A2, accession #NM_053380.2, 856 bp), and NaPi-IIc (SLC34A3, accession # NM_139338.1 , (1) 513 bp, (2) 786 bp). **(A)** RT-PCR was conducted in the kidney where NaPi-IIa and NaPi-IIc are known to occur. **(B)** The gut has been reported to have NaPi-IIb-type transporters. Thus, RT-PCR analysis was performed in the rat gut as positive and negative controls for the NaPi-II isoforms.

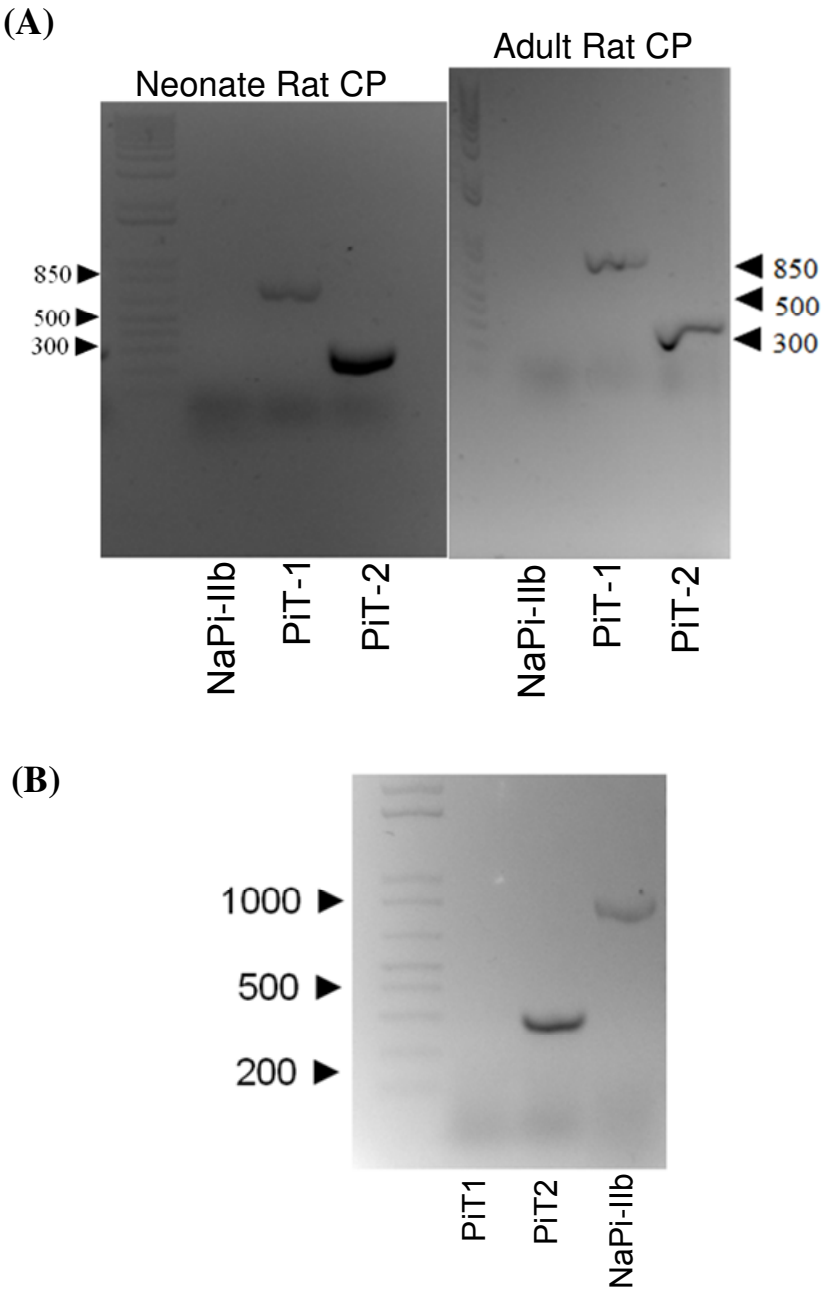

FIGURE 12. Semi-Quantitative RT-PCR Products of mRNA Extracted from Rat CP.
(A) Total mRNA was extracted from adult and neonate rat choroid plexus epithelium in primary cultures, compliments of Dr. Alice Villalobos. The adult rat choroid plexus was from the IV ventricle. NaPi-IIb (SLC34A2, accession #NM_053380.2, 856 bp), PiT1 (SLC20A1, accession # NM_031148.1, 758 bp), and PiT2 (SLC20A2, accession # NM_017223.2, 337 bp) mRNA primers were used. **(B)** Primers were designed against NaPi-IIb, PiT1, and PiT2 mRNA and used in RT-PCR analysis in adult rat choroid plexus.

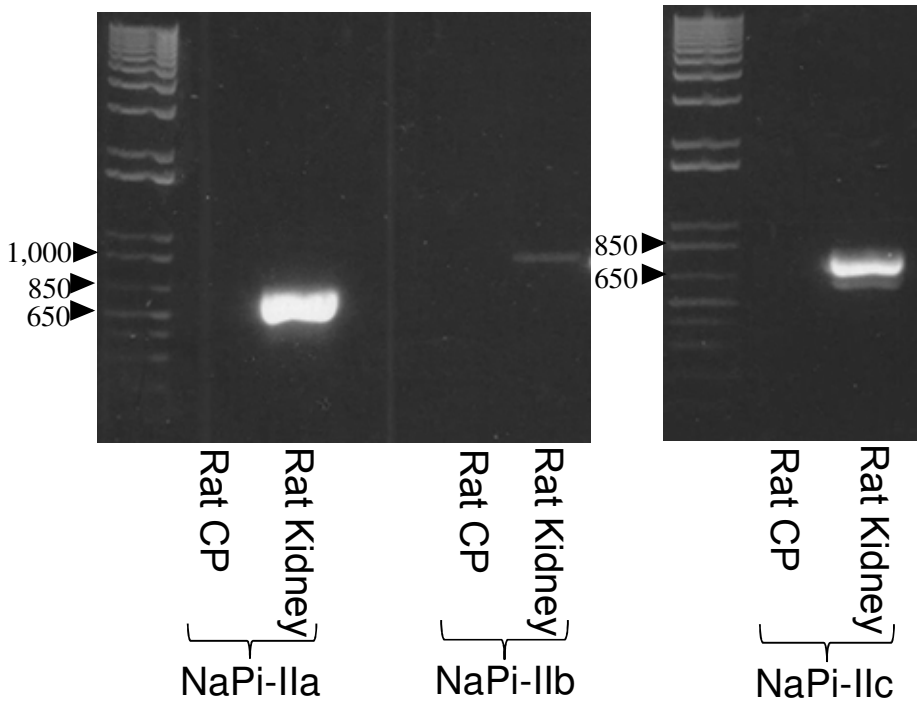

FIGURE 13. Semi-Quantitative RT-PCR Products of mRNA Extracted from Rat Choroid Plexus and Rat Kidney. All three NaPi-II isoform primers were used in RT-PCR analysis of rat kidney and rat CP. Rat kidney was used as a positive control for NaPi-IIa and NaPi-IIc but acted as a negative control for NaPi-IIb. (NaPi-IIa: 630 bp, NaPi-IIb: 856 bp, NaPi-IIc: 786 bp)

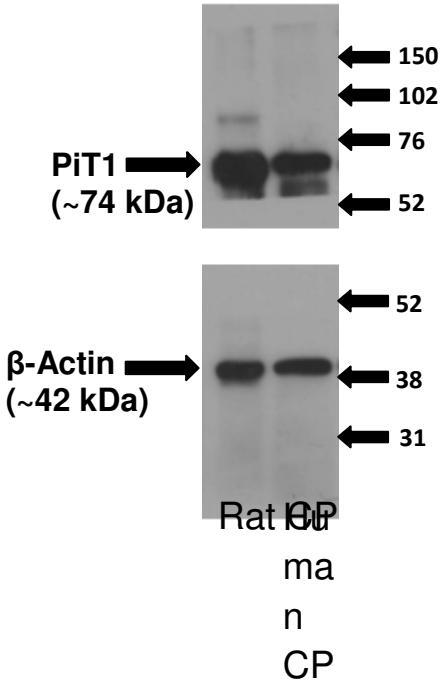

FIGURE 14. Western Blot Analysis of PiT1 Transporter Expression in Intact Rat and Human CP tissue. Rat and human choroid plexus cell proteins were separated by SDS-PAGE electrophoresis and transferred to a PVDF membrane. The membranes were probed with primary rabbit anti-PiT1 (Santa Cruz Biotechnology) and rabbit anti-β and stained with the secondary antibody, goat anti-rabbit HRP-conjugated IgG. Bands were visualized by ECL luminescence. PiT1 (74 kDa), β-Actin (~42 kDa)

FIGURE 15.

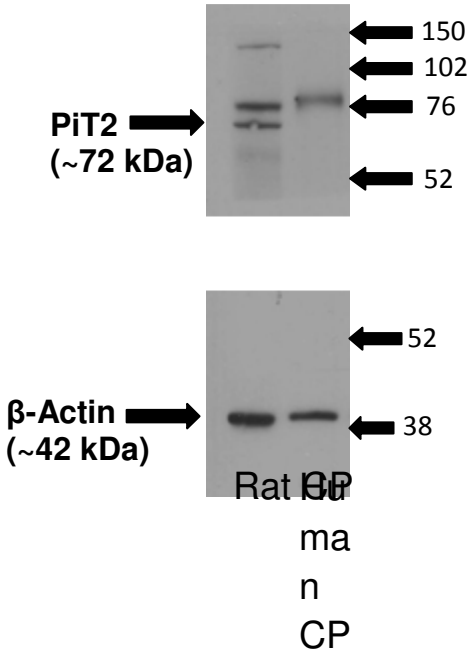

FIGURE 15. Western Blot Analysis of PiT2 Expression in Rat and Human Choroid Plexus Cells. 40 µg samples of rat and human choroid plexus cells were loaded and separated by 12% SDS-PAGE gel electrophoresis. Immunoblots were stained with either PiT2 (From Sorribas, et. al., ~72 kDa) or β-actin primary antibody (~42 kDa) and then secondary antibody (goat anti-rabbit Hrp-conjugated IgG). Bands were detected by ECL luminescence.

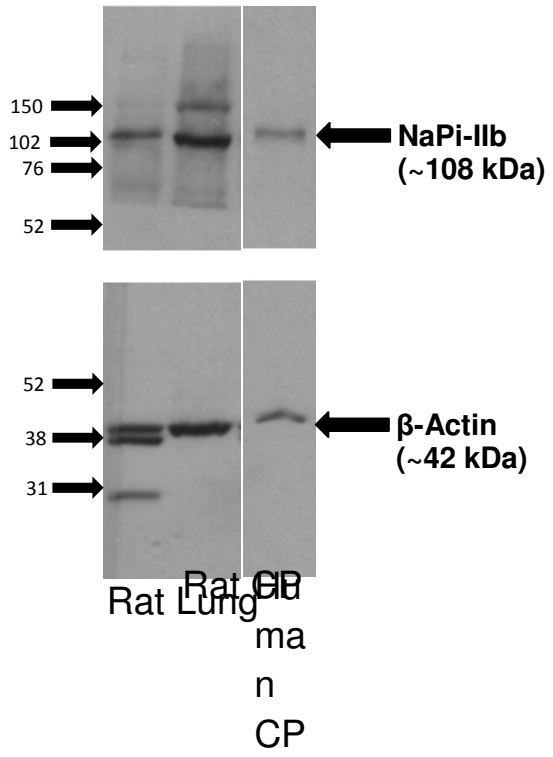

FIGURE 16. Western Blot Analysis of NaPi-IIb Expression in Rat and Human Choroid Plexus Cells. Approximately 40 µg of intact rat and human choroid plexus cells were separated by electrophoresis on a 10% SDS-polyacrylamide gel and then transferred to a PVDF membrane. The top gel was incubated overnight with primary rat anti-NaPi-IIb (Abbiotec Biotechnology, ~108 kDa), whereas the bottom gel was incubated with rabbit anti-β-actin (~42 kDa) for two hours. ECL luminescence was used to visualize bands. Rat lung tissue was used as a positive control.

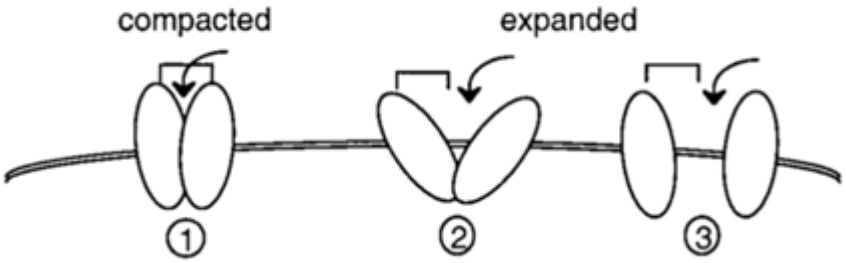

FIGURE 17. Schematic Representation of the Configuration of Cell Surface PiT2 Assemblies at Various [P_i] by Salaün et al. At low [P_i], PiT2 assemblies are in a "compact" configuration, which allows cross-linking of monomers. This configuration mediates active P_i uptake. (2, 3) At higher [P_i], PiT2 assemblies are in a relaxed configuration. The distance between the monomers allows efficient cross-linking and is associated with inactive P_i uptake.

FIGURE 18. Proposed Model of P_i Transport in Choroid Plexus Cells. Green= PiT2, Red= Na^+-K^+-ATPase, Purple= Unknown Basolateral P_i Transporter, Blue= AE2

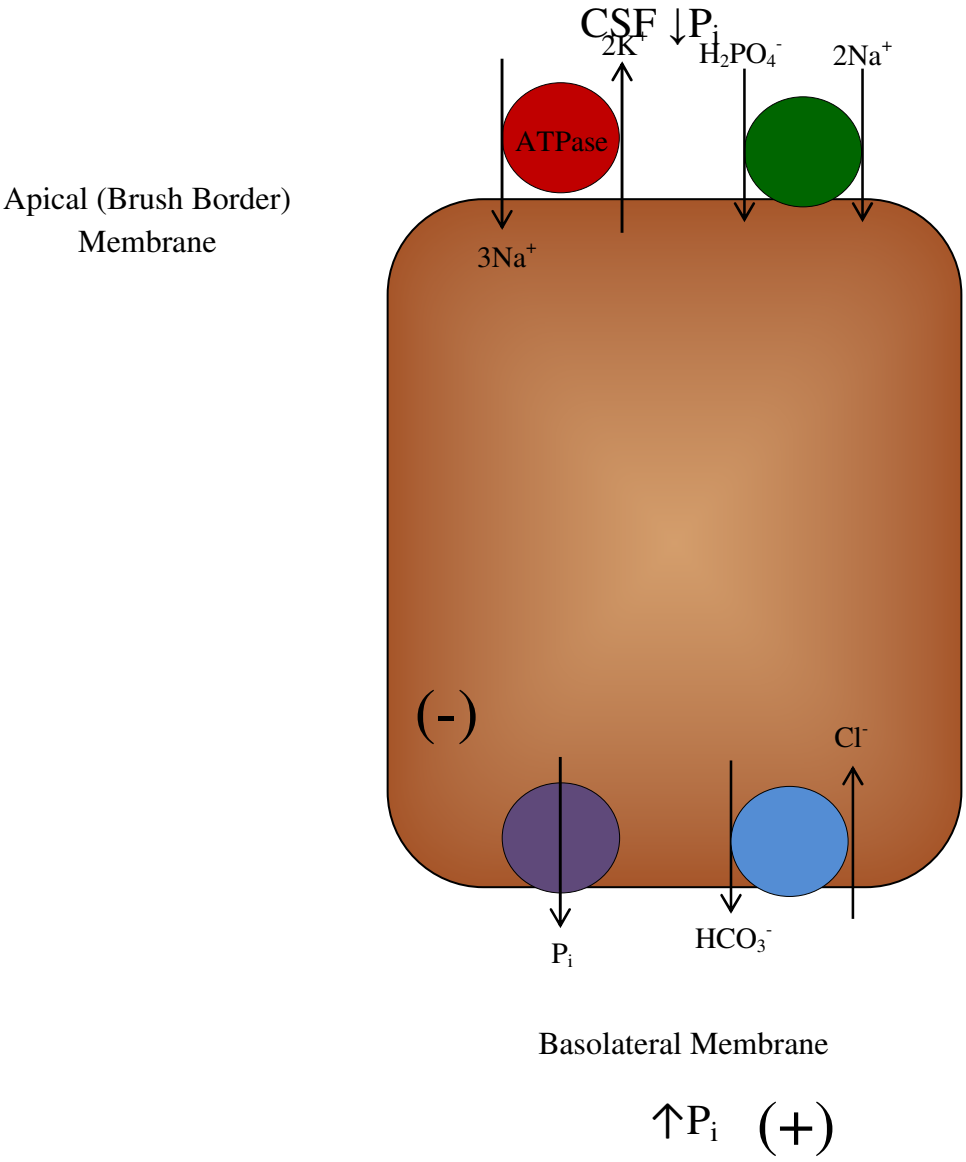

Table 1. Properties of Sodium-Dependent Phosphate Transporters by Virkki et. al. (2007)(Virkki et al., 2007)

Na^+/P_i Cotransporters	Substrates	Stoichiometry Na^+/P_i	Electrogenic	PFA Block
NaPi-IIa	Na^+, HPO_4^{2-}, Arsenate	3:1	Yes	Yes
NaPi-IIb	Na^+, HPO_4^{2-}, Arsenate	3:1	Yes	Yes
NaPi-IIc	Na^+, HPO_4^{2-}, Arsenate	2:1	No	Yes
PiT-1	Na^+, $H_2PO_4^-$, Li^+, Arsenate	2:1	Yes	No
PiT-2	Na^+, $H_2PO_4^-$, Li^+, Arsenate	2:1	Yes	No

TABLE 2. Nucleotide Sequence, Nucleotide Correspondence and Fragment Size of Primers used in RT-PCR Amplification.

Primer Name	Nucleotide Sequence	Nucleotide Correspondence	Amplified Fragment Size
SLC34A1_For	5'-TCC AGC ACC TCG ACA TCC ATC ATT-3'	540	630
SLC34A1_Rev	5'-TGA GCA CAG CGT ATG ACT ATG GCA-3'	1146	630
SLC34A2_For	5'-TGA GCA CAG CGT ATG ACT ATG GCA-3'	2202	856
SLC34A2_Rev	5'-TGA GCA CAG CGT ATG ACT ATG GCA-3'	3035	856
SLC34A3_For (1)	5'-TGA GAA ATG CAG GGA CCT CTG GTT-3'	162	513
SLC34A3_Rev (1)	5- AAG GCC CTC TGA AAT TCA TCC CGA-3'	651	513
SLC34A3_For (2)	5'-AAG GCA CTG ACT CGA CCT TTC ACA-3'	803	786
SLC34A3_Rev (2)	5'-AGA CAA TGG CTA CCC AGC GGT ATT-3'	1565	786
SLC20A1_For	5'- CAA ACA TTG GCC TTC CCA TCA GCA-3'	1898	758
SLC20A1_Rev	5'- TGC CAA AGA TTC TCG GCC CTC TAA-3'	2633	758
SLC20A2_For	5'-TGC AGT GGA TGG AAC TCG TCA AGA-3'	818	337
SLC20A2_Rev	5'-TCT TCA TCC ACG GAC ACA CGA ACA-3'	1132	337

REFERENCES

1. **Brown SB, Bailey K, Savill J**. Actin is cleaved during constitutive apoptosis. [Online]. *The Biochemical journal* 323 (Pt 1): 233-7, 1997.

2. **Béliveau R, Dallaire L, Giroux S**. Phosphate transport in capillaries of the blood-brain barrier. [Online]. *Advances in experimental medicine and biology* 331: 75-80, 1993.

3. **Bøttger P, Hede SE, Grunnet M, Høyer B, Klaerke D a, Pedersen L**. Characterization of transport mechanisms and determinants critical for Na+-dependent Pi symport of the PiT family paralogs human PiT1 and PiT2. *American journal of physiology. Cell physiology* 291: C1377-87, 2006.

4. **Collins JF, Bai L, Ghishan FK**. The SLC20 family of proteins: dual functions as sodium-phosphate cotransporters and viral receptors. *Pflügers Archiv□: European journal of physiology* 447: 647-52, 2004.

5. **Cornford EM, Varesi JB, Hyman S, Damian RT, Raleigh MJ**. Mitochondrial content of choroid plexus epithelium. [Online]. *Experimental brain research. Experimentelle Hirnforschung. Expérimentation cérébrale* 116: 399-405, 1997.

6. **Cserr F, Island R**. Physiology of the Choroid Plexus. *Perfusion* 61, 1971.

7. **Damkier HH, Brown PD, Praetorius J**. Epithelial pathways in choroid plexus electrolyte transport. *Physiology (Bethesda, Md.)* 25: 239-49, 2010.

8. **Hashimoto M, Wang D-yu**. Short Communication Isolation and Localization of Type IIb Na / Pi Cotransporter in the Developing Rat Lung. *Cellular & Molecular Biology (Oxford)* 157: 21-27, 2000.

9. **Eijkman C, Indies DE, Funk C, States U, East F, Iv P, States U**. PART IV The Nutrients – Deficiencies , Surfeits , and Food-Related Disorders. *Online*.

10. **Johanson CE, Duncan J a, Klinge PM, Brinker T, Stopa EG, Silverberg GD**. Multiplicity of cerebrospinal fluid functions: New challenges in health and disease. *Cerebrospinal fluid research* 5: 10, 2008.

11. **Kayalar C, Ord T, Testa MPIA, Zhong L-tao, Bredesen DE**. Cleavage of actin by interleukin 1 (3-converting DNase I inhibition reverse. *Nature* 93: 2234-2238, 1996.

12. **Lau WL, Festing MH, Giachelli CM**. Phosphate and vascular calcification: Emerging role of the sodium-dependent phosphate co-transporter PiT-1. *Thrombosis and haemostasis* 104: 464-70, 2010.

13. **Lowery LA, Sive H**. Totally tubular: the mystery behind function and origin of the brain ventricular system. *BioEssays□: news and reviews in molecular, cellular and developmental biology* 31: 446-58, 2009.

14. **Di Marco GS, Hausberg M, Hillebrand U, Rustemeyer P, Wittkowski W, Lang D, Pavenstädt H**. Increased inorganic phosphate induces human endothelial cell apoptosis in vitro. *American journal of physiology. Renal physiology* 294: F1381-7, 2008.

15. **Miyamoto K-ichi, Ito M, Tatsumi S, Kuwahata M, Segawa H**. New aspect of renal phosphate reabsorption: the type IIc sodium-dependent phosphate transporter. *American journal of nephrology* 27: 503-15, 2007.

16. **Miyamoto K-ichi, Segawa H, Ito M, Kuwahata M**. Physiological regulation of renal sodium-dependent phosphate cotransporters. [Online]. *The Japanese journal of physiology* 54: 93-102, 2004.

17. **Murer, Heini, and Jurg Biber.** "Phosphate Transport in the Kidney." *Journal of Nephrology*23 (2010): S145-151. Print.

18. **Murer H, Forster I, Biber J**. The sodium phosphate cotransporter family SLC34. *Pflügers Archiv□: European journal of physiology* 447: 763-7, 2004.

19. **Ohi A, Hanabusa E, et al**. Inorganic phosphate homeostasis in sodium-dependent phosphate cotransporter Npt2b + / − mice Inorganic phosphate homeostasis in sodium-dependent phosphate. *Renal Physiology* (2012).

20. **Ohnishi R, Segawa H, Kawakami E, Furutani J, Ito M, Tatsumi S, Kuwahata M, Miyamoto K-I**. Control of phosphate appetite in young rats. [Online]. *The journal of medical investigation□: JMI* 54: 366-9, 2007.

21. **Porterfield, Susan P., and Bruce Alan. White.** "Calcium and Phosphate Homeostasis."*Endocrine Physiology*. Philadelphia, PA: Mosby/Elsevier, 2007. 81-82. Print.

22. **Prié D, Ureña Torres P, Friedlander G**. Latest findings in phosphate homeostasis. *Kidney international* 75: 882-9, 2009.

23. **Redzic ZB, Segal MB**. The structure of the choroid plexus and the physiology of the choroid plexus epithelium. *Advanced drug delivery reviews* 56: 1695-716, 2004.

24. **Renkema KY, Alexander RT, Bindels RJ, Hoenderop JG**. Calcium and phosphate homeostasis: concerted interplay of new regulators. *Annals of medicine* 40: 82-91, 2008.

25. **Sabbagh, Yves, Hector Giral, Yupanqui Caldas, Moshe Levi, and Susan C. Schiavi.** "Intestinal Phosphate Transport." *Advances in Chronic Kid ney Disease* 18.2 (2011): 85-90. Print.

26. **Salaün C, Gyan E, Rodrigues P, Heard JM**. Pit2 Assemblies at the Cell Surface Are Modulated by Extracellular Inorganic Phosphate Concentration. *Society* 76: 4304-4311, 2002.

27. **Segawa H, Kaneko I, Takahashi A, Kuwahata M, Ito M, Ohkido I, Tatsumi S, Miyamoto K-I**. Growth-related renal type II Na/Pi cotransporter. *The Journal of biological chemistry* 277: 19665-72, 2002.

28. **Serot J-M, Zmudka J, Jouanny P**. A Possible Role for CSF Turnover and Choroid Plexus in the Pathogenesis of Late Onset Alzheimer's Disease. *Journal of Alzheimer's disease□: JAD* 28: 1-10, 2012.

29. **Silverthorn, Dee Unglaub.** *Human Physiology: an Integrated Approach*. San Francisco: Pearson Benjamin Cummings, 2010. 672-74. Print.

30. **Stoff, J.** "Phosphate Homeostasis and Hypophosphatemia." *The American Journal of Medicine* 72.3 (1982): 489-95. Print.

31. **Villa-Bellosta R, Bogaert YE, Levi M, Sorribas V**. Characterization of phosphate transport in rat vascular smooth muscle cells: implications for vascular calcification. *Arteriosclerosis, thrombosis, and vascular biology* 27: 1030-6, 2007.

32. **Villalobos AR a, Miller DS, Renfro JL**. Transepithelial organic anion transport by shark choroid plexus. *American journal of physiology. Regulatory, integrative and comparative physiology* 282: R1308-16, 2002.

33. **Virkki LV, Biber J, Murer H, Forster IC**. Phosphate transporters: a tale of two solute carrier families. *American journal of physiology. Renal physiology* 293: F643-54, 2007.

34. **Wolburg H, Paulus W**. Choroid plexus: biology and pathology. *Acta neuropathologica* 119: 75-88, 2010.